Research Article

Wall shear stress is decreased in the pulmonary arteries of patients with pulmonary arterial hypertension: An image-based, computational fluid dynamics study

Beverly T. Tang[1], Sarah S. Pickard[2], Frandics P. Chan[3], Philip S. Tsao[4], Charles A. Taylor[1,5], and Jeffrey A. Feinstein[5,6]

Departments of [1]Mechanical Engineering, Stanford University, [2]Pediatrics, Harvard University, Boston, Massachusetts, [3]Radiology, [4]Medicine, [5]Bioengineering, and [6]Pediatrics (Cardiology), Stanford University, Stanford, California, USA

ABSTRACT

Previous clinical studies in pulmonary arterial hypertension (PAH) have concentrated predominantly on distal pulmonary vascular resistance, its contribution to the disease process, and response to therapy. However, it is well known that biomechanical factors such as shear stress have an impact on endothelial health and dysfunction in other parts of the vasculature. This study tested the hypothesis that wall shear stress is reduced in the proximal pulmonary arteries of PAH patients with the belief that reduced shear stress may contribute to pulmonary endothelial cell dysfunction and as a result, PAH progression. A combined MRI and computational fluid dynamics (CFD) approach was used to construct subject-specific pulmonary artery models and quantify flow features and wall shear stress (WSS) in five PAH patients with moderate-to-severe disease and five age- and sex-matched controls. Three-dimensional model reconstruction showed PAH patients have significantly larger main, right, and left pulmonary artery diameters (3.5 ± 0.4 vs. 2.7 ± 0.1 cm, $P = 0.01$; 2.5 ± 0.4 vs. 1.9 ± 0.2 cm, $P = 0.04$; and 2.6 ± 0.4 vs. 2.0 ± 0.2 cm, $P = 0.01$, respectively), and lower cardiac output (3.7 ± 1.2 vs. 5.8 ± 0.6 L/min, $P = 0.02$.). CFD showed significantly lower time-averaged central pulmonary artery WSS in PAH patients compared to controls (4.3 ± 2.8 vs. 20.5 ± 4.0 dynes/cm^2, $P = 0.0004$). Distal WSS was not significantly different. A novel method of measuring WSS was utilized to demonstrate for the first time that WSS is altered in some patients with PAH. Using computational modeling in patient-specific models, WSS was found to be significantly lower in the proximal pulmonary arteries of PAH patients compared to controls. Reduced WSS in proximal pulmonary arteries may play a role in the pathogenesis and progression of PAH. This data may serve as a basis for future in vitro studies of, for example, effects of WSS on gene expression.

Key Words: biomedical engineering, computer simulation, endothelium-derived factors

Pulmonary arterial hypertension (PAH) is a chronic disease characterized by progressive elevation in pulmonary artery pressure due to increased resistance in the distal pulmonary arteries and decreased compliance in the proximal arteries. If left untreated, PAH patients have a median survival of less than three years from the time of diagnosis,[1,2] often attributable to the resulting compromised right ventricular function. A known mechanism of endothelial dysfunction in the systemic circulation is reduction in wall shear stress (WSS); however, little is known about pulmonary endothelial cell-specific responses to these forces and their role in the pathogenesis and progression of pulmonary vascular diseases, such as PAH.[3,4] It has been proposed that pulmonary vascular endothelial dysfunction may play a large role in the pathogenesis of PAH,[5-9] including the medial thickening, intimal fibrosis, microthrombosis, and plexiform lesions that affect the pre-capillary pulmonary arteries.

Address correspondence to:
Dr. Jeffrey A. Feinstein
Lucile Packard Children's Hospital
Stanford University Medical Center
750 Welch Road, Suite 305
Palo Alto, CA 94304-5731, USA
Email: jeff.feinstein@stanford.edu

Access this article online	
Quick Response Code:	**Website:** www.pulmonarycirculation.org
	DOI: 10.4103/2045-8932.105035
	How to cite this article: Tang BT, Pickard SS, Chan FP, Tsao PS, Taylor CA, Feinstein JA. Wall shear stress is decreased in the pulmonary arteries of patients with pulmonary arterial hypertension: An image-based, computational fluid dynamics study. Pulm Circ 2012;2:470-6.

Previous clinical studies have concentrated on the properties of the distal vasculature in PAH, its contribution to the disease process, and its response to therapy. Specifically, pulmonary vascular resistance is routinely measured and used as a guide for therapeutic efficacy and therapy escalation.[10,11] Ventricular loading, however, is dependent on both resistance and total arterial compliance.[12-14] Decreased compliance associated with PAH and changes in response to vasodilators have been demonstrated in patients with PAH.[15,16] Despite this and other compelling evidence that pulmonary artery compliance is a significant factor in decoupling the right ventricle from its vascular load,[17,18] few clinical investigations to date have looked at biomechanical factors, such as wall shear stress, in the central pulmonary arteries in PAH,[19] and none have examined their potential to offer insight into disease severity and outcomes.

The ability to accurately measure WSS through the combination of MRI and computational fluid dynamics (CFD) is a novel development. WSS, measured in dynes/cm^2, is a frictional force along the inner wall of the artery caused by viscous drag. Unlike ultrasound, which only measures one component of velocity, CFD allows for the creation of a time-varying 3D velocity field within the lumen. CFD facilitates analysis of flow patterns, spatial distribution of velocity, turbulence, and WSS in a diseased state. To improve accuracy in the setting of complex geometry, "meshing" is used, in which the arterial geometry is broken down into smaller components, such as tetrahedrons.[20] High-resolution 3D imaging, such as gadolinium-enhanced magnetic resonance angiography, combined with CFD, enable accurate assessment of WSS in the pulmonary vasculature as previously demonstrated.[21]

We hypothesize that the abnormal anatomic and hemodynamic properties of the central pulmonary arteries will lead to a decrease in WSS which, as demonstrated in the systemic circulation, may lead to pulmonary endothelial cell dysfunction and abnormal gene expression. As a first step toward elucidating the role of shear stress in the pathogenesis and progression of PAH, we combined MRI and computational fluid dynamics to construct subject-specific pulmonary artery models in five PAH patients and five age- and sex-matched controls in order to quantify WSS and provide a basic range of normal WSS for future studies.

MATERIALS AND METHODS

Magnetic resonance imaging

Gadolinium-enhanced magnetic resonance angiography (MRA) scans of five subjects with PAH (16- and 41-year-old males, and 19-, 36- and 50-year-old females) and five age- and sex-matched healthy subjects in the supine position were obtained in a 1.5T GE Signa MR scanner (GE Medical Systems, Milwaukee, Wisc.). IRB-approved informed consent was obtained from all subjects. Gadopentetate dimeglumine contrast agent (Magnevist, Bayer HealthCare, Wayne, N.J.) 0.2 mmol/kg was injected at a rate of 2 mL/sec via antecubital intravenous access, and a three-dimensional fast gradient echo MRA sequence was used to obtain a volume of coronal slices in 20 seconds during one breath-hold. Slice thickness ranged from 3.0 to 3.2 mm, interpolated to 1.5 to 1.6 mm, totaling 50 to 60 slices per volume. A 512 × 192 acquisition matrix (reconstructed to 512 × 512) was used with an in-plane field of view of 35 × 35 cm^2 to provide an in-plane reconstructed spatial resolution of 0.68 mm. The true imaging resolution of the MRA scans was 0.7 × 1.8 × 3.0 mm while the interpolated image voxel size was 0.7 × 0.7 × 1.5 mm. Other scan parameters included repetition times (TR) of 2.7 to 3.5 milliseconds, echo times (TE) of 0.704 to 0.844 ms, and flip angles of 25°.

During the same imaging study, breath-held, segmented k-space phase contrast cine images with through-plane velocity encoding were obtained perpendicular to the main (MPA), left (LPA), and right (RPA) pulmonary arteries. This series of images provided subject-specific physiologic flow information at the three locations. The acquisitions were ECG-gated, with TR = 2.2-2.5 ms and eight views per segment, resulting in a temporal resolution of 40 ms. Twenty time points evenly spaced within a cardiac cycle were retrospectively reconstructed. Through-plane velocities were measured through 10-mm thick slices with velocity encoding gradients of 150 cm/seconds to 250 cm/seconds. Other imaging parameters included 28 or 30 square cm field of views, a 256 × 160 acquisition matrix yielding an in-plane resolution of 1.1 × 1.8 mm, 4.4 to 4.7 ms TRs, 2.2 to 2.5 ms TEs, and 15° or 20° flip angles.

Image processing, model construction and boundary condition specification

In each volume of MRA data acquired, geometric distortions caused by magnetic gradient nonlinearity were corrected to preserve the true dimensions of the pulmonary vasculature.[22] Three-dimensional, subject-specific solid models of the pulmonary tree were created from the MRA images using custom software[23] and discretized into a coarse, isotropic mesh using a commercially available, automatic mesh generation program (MeshSim, Simmetrix, Clifton Park, N.Y.).

The cine phase contrast images (PC-MRI) taken perpendicularly to the main, left, and right pulmonary arteries were used to calculate in vivo, time-resolved volumetric flow. For each of the 20 time points, the lumen of the respective vessels was determined from the intensity magnitude images using a level set method,[24] and through-plane velocity values for each pixel were

integrated over the bounded area to calculate a total volume flow rate.[22] The periodic flow waveform at the MPA was mapped onto the inlet face using a parabolic profile, and the average volumetric flow calculated from the PC-MRI for the left and right pulmonary arteries was used to determine the flow split to each side. Resistance values were assigned at the outlet of each branch vessel based on the area of the outlet, the LPA/RPA flow split, and either healthy pressure values (average of 12 mmHg) for the healthy subjects or subject-specific pressure values measured from catheterization in the PAH subjects. Furthermore, a rigid wall assumption and a no-slip boundary condition at the wall were also prescribed.

Once all boundary conditions were applied, the flow solution for each subject-specific mesh was obtained using a stabilized finite element method to solve the incompressible Navier-Stokes equations.[25] Each coarse, isotropic mesh was then adaptively refined into an anisotropic mesh based on the results of the solution (in order to reduce local error), and this process was repeated until mesh independence was reached. The resulting refined subject-specific meshes contained an average size of 1.2 million tetrahedral elements.

Analysis of simulation results

From the simulation results, time-averaged wall shear stress (τ_{mean}) was computed for each subject. τ_{mean} is defined as the magnitude of the time-averaged surface traction vector, t_s, which is the tangential component of the traction vector, t.

$$\tau_{mean} = \left| \frac{1}{T} \int_0^T t_s \right|$$

where:

$$t_s = t - (t \bullet n)n$$

and:

$$t = \sigma n$$

where s is the stress tensor, n is the surface normal vector, and T is the period of the cardiac cycle.

In order to quantitatively analyze and compare the mean wall shear stress for all subjects, 10-mm strips were taken perpendicularly around the circumference of the LPA and RPA before the first branch, as well as at a random selection of distal branch vessels (three vessels on each side with cross-sectional area of 10-mm^2), and values were averaged over the surface area. Mean wall shear stress was statistically compared using a student's *t*-test with significance set at $P < 0.05$.

RESULTS

Anatomic and hemodynamic features of PAH

Three-dimensional model construction of the large pulmonary arteries and major branches illustrated the anatomic differences between healthy, normal subjects, and PAH patients. As predicted, PAH patients were observed to have more tortuous branch vessels and larger proximal arteries, with an average main pulmonary artery diameter of 3.5 ± 0.4 cm (compared to 2.7 ± 0.1 cm in healthy subjects, $P = 0.01$), right pulmonary artery diameter of 2.5 ± 0.4 cm (compared to 1.9 ± 0.2 cm in healthy subjects, $P = 0.04$), and left pulmonary artery diameter of 2.6 ± 0.4 cm (compared to 2.0 ± 0.2 cm in healthy subjects, $P = 0.01$). Additional subject data collected during the study is summarized in Table 1.

Flow rate (i.e., cardiac output) measured at the MPA was significantly lower in the PAH patients (3.7 ± 1.2 L/min (2.0 L/m/m^2) compared to 5.8 ± 0.6 L/min (3.3 L/m/m^2 in healthy subjects, $P = 0.02$). The combination of larger proximal arteries and lower flow rates in the PAH patients led to lower velocity magnitude and more stagnant flow throughout the cardiac cycle in the proximal arteries of the PAH patients. A volume-rendered plot of velocity

Table 1: Subject-specific MRI and catheterization data

	Subject	Age	Sex	BSA (m^2)	MRI data		Cardiac catheterization data		
					MPA diameter (cm)	MPA flow (L/min)	RA_p (mean, mm Hg)	PA_p (S/D, M; mm Hg)	PVRI (U/m^2)
PAH patients	1	16	M	1.55	3.2	2.6	4	70/37, 50	10.7
	2	19	F	1.58	3.1	2.4	7	95/45, 67	21.5
	3	36	F	2.16	3.2	5.2	4	87/36, 50	22.9
	4	41	M	1.87	3.7	4.4	4	77/30, 49	18.1
	5	50	F	2.00	4.1	3.8	7	110/42, 68	37.2
Controls		21	M	1.76	2.7	6.0			
		22	F	1.66	2.7	5.1			
		31	F	1.60	2.6	5.4			
		35	M	2.00	2.6	6.6			
		51	F	1.75	2.8	5.9			

MPA: main pulmonary artery; **RA_p:** right atrial pressure; **PA_p:** Pulmonary artery pressure (systolic/diastolic, mean); **PVR:** pulmonary vascular resistance (Woods units)

magnitude in the pulmonary arteries of one representative PAH patient and an age- and sex-matched normal subject is shown in Figure 1. Note that, even at peak systole, the velocity magnitude in the proximal pulmonary arteries of the PAH patient was very low, and almost no flow movement was observed throughout diastole. In comparison, the velocity magnitude was consistently higher in the pulmonary arteries of the normal control subject at similar time points during the cardiac cycle. A more detailed look at the cross-sectional flow features in the LPA and RPA of these two subjects is shown in Figure 2. A low-intensity, more uniform flow field was observed in the PAH patient whereas high-intensity, swirling flow along the walls of the proximal arteries was found in the normal control subject.

Mean wall shear stress (WSS) results are summarized for all subjects in Figure 3. Plots of mean WSS illustrate that PAH subjects have lower mean WSS in their proximal arteries compared to healthy subjects. In many subjects, areas of low mean WSS were found at sites opposite to branch points, indicating possible recirculation zones in these regions. However, it should be noted that the levels of low mean WSS in the proximal pulmonary arteries of the control subjects is still higher than the overall levels found in the PAH patients. When quantified using 10-mm strips taken around the circumference, the mean WSS of the proximal pulmonary arteries of healthy subjects was nearly five times higher than that of the PAH patients (20.5 ± 4.0 dynes/cm^2 in the control subjects compared to 4.3 ± 2.8 dynes/cm^2 in the PAH patients, P = 0.0004). Mean WSS values in the distal arteries was 1.4 times higher in the normal subjects than the PAH patients (14.1 ± 0.7 dynes/cm^2 in the control subjects compared to 10.1 ± 0.9 dynes/cm^2 in the PAH patients, P = 0.004).

DISCUSSION

Altered systemic shear stress has been shown to have a detrimental effect on cardiovascular health. As an initial step in elucidating whether similar biomechanical forces adversely affect pulmonary vascular health, we quantified the mean WSS in patients with PAH as compared to age- and sex-matched controls. We found significantly lower wall shear stress in the pulmonary arteries of five subjects with moderate or severe PAH compared to control subjects using combined magnetic resonance imaging and computational fluid dynamics to visualize and quantify subject-specific, three-dimensional hemodynamic conditions. This study also provides novel insight into the time-varying blood flow features that exist in the pulmonary vasculature in health and disease and suggests a mechanism by which conditions of low shear stress may result in disease progression.

Numerous secondary observations can be made about alterations in velocity and flow in the pulmonary vasculature of PAH. The swirling, high-wall-velocity flow noted in normal subjects at rest did not occur in PAH

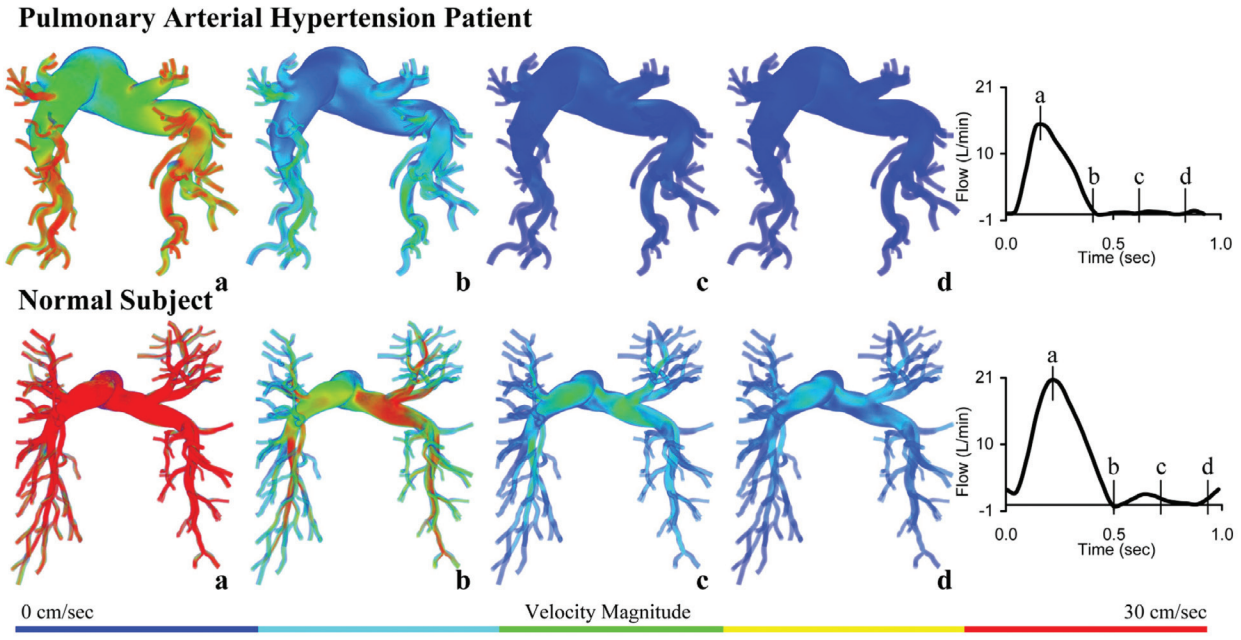

Figure 1: Volume-rendered velocity magnitudes plotted in the pulmonary arteries of a 50-year-old female with Pulmonary Arterial Hypertension (top) and a 51-year-old healthy female volunteer (bottom). The left-most panel shows peak-systole for both subjects, and equally-spaced time points throughout the cardiac cycle are shown in the following three panels.

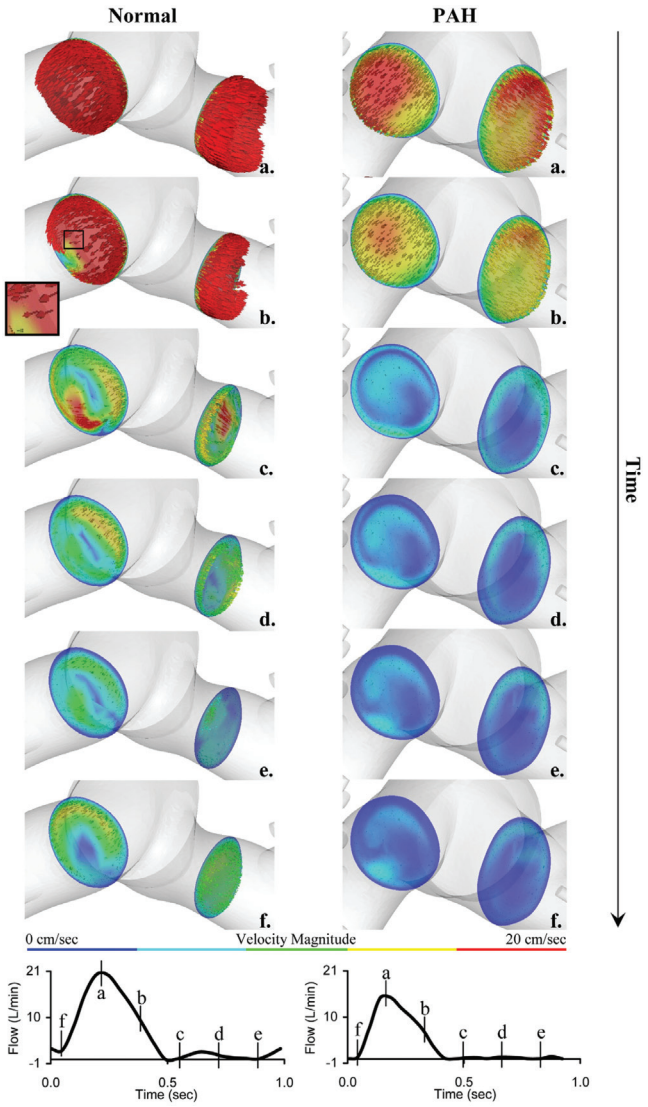

Figure 2: Cross-sectional view of flow features in the LPA and RPA of the PAH patient (right) and the age- and sex-matched normal control subject (left) featured in Figure 1. Arrowheads (shown enlarged in inset of panel b) are used to represent velocity vectors and are colored and scaled according to velocity magnitude. In addition, velocity magnitude is plotted on a cross sectional slice through the vessel.

patients, thus leading to significantly lower wall shear stresses. The most notable difference in flow features between a PAH patient and a normal subject, as shown in Figures 2 and 3, are the higher, swirling velocities along the wall in the normal subject. In comparison, flow is basically stagnant for more than half of the cardiac cycle in the PAH patient, with higher flow velocities along the wall only occurring at peak systole. These higher flow velocities along the walls of the proximal vessels in normal subjects led to an overall six times higher wall shear stress than in PAH patients when compared across all subjects. Interestingly, this difference in wall shear stress was diminished in the distal vasculature, likely due to pruning of the distal arteries, thus leading to similar distributions of flow.

It has been extensively demonstrated in the systemic circulation that wall shear stress modulates endothelial function. Specifically, systemic increases in WSS result in elevated expression of eNOS.[3,26-28] Nitric oxide is also a primary modulator of pulmonary vasodilation and target of PAH drug therapies, such as sildenafil.[29-32] In addition, WSS alters pulmonary expression of Hsp90, an activator of eNOS, NAD(P)H dehydrogenase quinone 1, an antioxidant, monocyte-chemotactic protein 1, and platelet endothelial cell adhesion molecule 1.[28,33-36] Reduction in angiotensin-converting enzyme has also been shown with increases in pulmonary vasculature shear stress.[37] Therefore, one could conclude that dramatic changes in the WSS of the pulmonary vasculature, as we demonstrated in PAH, would have significant effects on pulmonary endothelial health and remodeling.

Our findings may elucidate one of the mechanisms by which epoprostenol improves patient outcomes, results in long-term reductions of pulmonary vascular resistance, and partially reverses disease progression.[38] Epoprostenol has been shown to significantly affect cardiac output and pulmonary vascular resistance and to cause long-term vasodilation despite lack of response to acute vasodilator testing. This may suggest a unique mechanism of action when given chronically.[38] We propose epoprostenol may alter wall shear stress in the pulmonary arteries by increasing cardiac output resulting in a positive remodeling response and long-term vasodilation. However, our current therapies at best stabilize but do not reverse the process. Perhaps this frustration is because we are combating two entities: the disease itself and the resulting abnormal biomechanical effects on the endothelium and gene expression. If shear stress is found to be a major determinant of and contributor to PAH, a target of future therapies may be alteration of the biomechanical environment as a means of reversing disease progression. Great interest now exists in using more aggressive therapy, e.g., epoprostenol, earlier in the disease treatment algorithm to get the most effect possible early on. This study may lend additional support to this proposed approach.

Clinically, assessment of wall shear stress by magnetic resonance, an imaging modality with increased utilization in clinical practice for the evaluation of right ventricular function, may serve to stratify disease severity and monitor the efficacy of existing and emerging therapies. Currently, symptomatology and PVR are the primary methods of assessing disease severity and response to therapy. However, measurement of WSS may prove to be a more comprehensive, non-invasive metric for tailoring therapy and determining prognosis.

The primary limitations of this study are the small number of patients and the severity of their disease. While there was

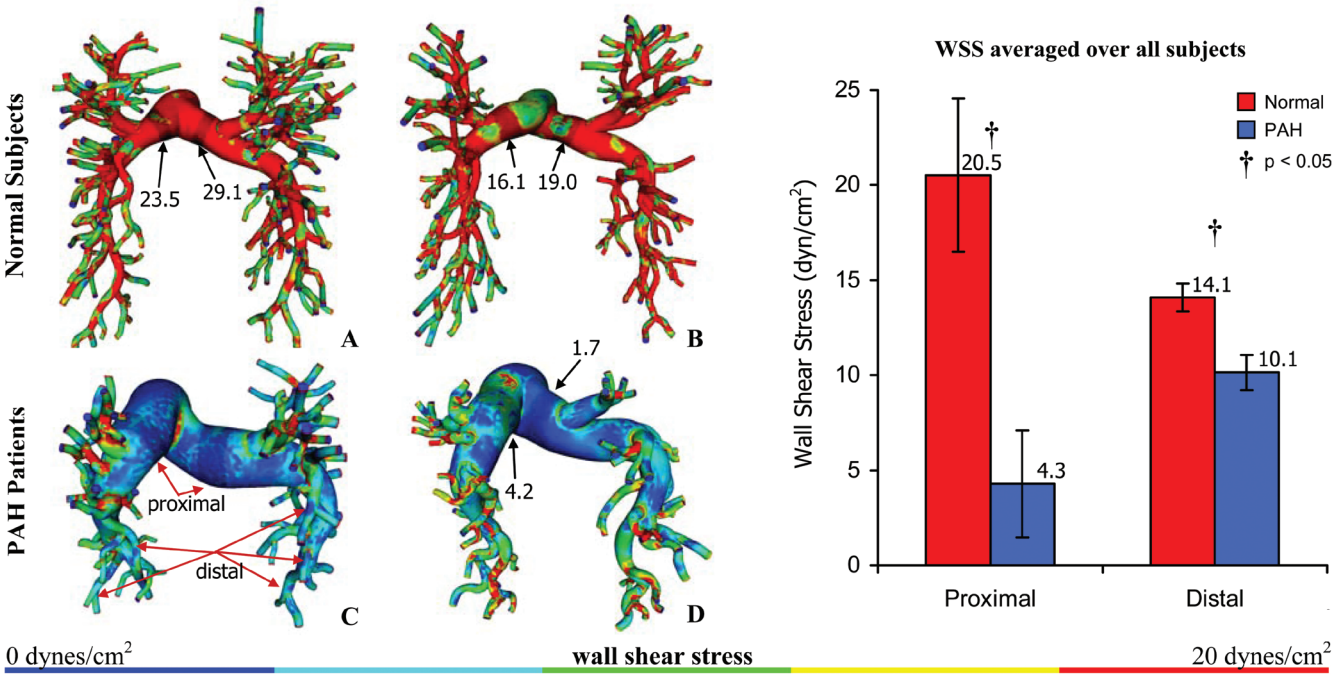

Figure 3: Summary of time-averaged wall shear stress (WSS) results for all subjects. Mean WSS color maps (left panel) for two representative age- and sex-matched (top) normal subjects and (bottom) PAH patients. Mean WSS was lower in the proximal arteries of the PAH patients than in those of the normal subjects. Mean WSS averaged over the area of 10-mm circumferential strips taken at the LPA and RPA (proximal) and distal locations was significantly different between the two populations (right panel).

an order of magnitude difference in WSS for each patient compared to control, this represents a small study of only five severe PAH patients. Of note, the broad age range of patients (16 to 50) was purposely chosen to increase the heterogeneity of the patient population and, therefore, improve possible applicability of findings. While this pilot study found a significant difference in WSS in PAH patients, and may lead to further advances in the basic science of this disease, future work must investigate the use of these non-invasive imaging and CFD techniques in a greater number of patients including a "healthier" PAH population to determine the sensitivity and specificity of these methods and clinical applicability.

This study represents the first time that three-dimensional hemodynamic conditions have been quantified in patient-specific models of pulmonary arterial hypertension and is an important step toward elucidating the role of shear stress in regulating pulmonary artery endothelial cell dysfunction. Our results point to a biomechanical mechanism as a component of pulmonary endothelial cell dysfunction and further progression of the disease. As distal resistance increases, flow is decreased in the enlarged proximal vessels, leading to decreased wall shear stress, which is known to negatively impact endothelial cell health. This shear-mediated endothelial dysfunction can lead to further remodeling of the proximal vessels, as well as downstream remodeling via endocrine signaling, resulting in worsening of the disease and further decreases in wall shear stress. All of these changes suggest a contribution of the unhealthy disease state to disease progression, that is, PH begets PH.

ACKNOWLEDGMENTS

The authors would like to thank Dr. Roham Zamanian, Juliana Liu, and Michelle Ogawa for their assistance in patient recruitment.

REFERENCES

1. D'Alonzo GE, Barst RJ, Ayres SM, Bergofsky EH, Brundage BH, Detre KM, et al. Survival in patients with primary pulmonary hypertension. Results from a national prospective registry. Ann Intern Med 1991;115:343-9.
2. Walcott G, Burchell HB, Brown AL Jr. Primary pulmonary hypertension. Am J Med 1970;49:70-9.
3. Fisher AB, Chien S, Barakat AI, Nerem RM. Endothelial cellular response to altered shear stress. Am J Physiol Lung Cell Mol Physiol 2001;281:L529-33.
4. Dudek SM, Garcia JG. Cytoskeletal regulation of pulmonary vascular permeability. J Appl Physiol 2001;91:1487-500.
5. Sitbon O, Gressin V, Speich R, Macdonald PS, Opravil M, Cooper DA, et al. Bosentan for the treatment of human immunodeficiency virus-associated pulmonary arterial hypertension. Am J Respir Crit Care Med 2004;170:1212-7.
6. Giaid A, Saleh D. Reduced expression of endothelial nitric oxide synthase in the lungs of patients with pulmonary hypertension. N Engl J Med 1995;333:214-21.
7. Giaid A, Yanagisawa M, Langleben D, Michel RP, Levy R, Shennib H, et al. Expression of endothelin-1 in the lungs of patients with pulmonary hypertension. N Engl J Med 1993;328:1732-9.
8. Archer S, Rich S. Primary pulmonary hypertension: A vascular biology and translational research "Work in progress." Circulation 2000;102:2781-91.
9. Botney MD. Role of hemodynamics in pulmonary vascular remodeling: Implications for primary pulmonary hypertension. Am J

Respir Crit Care Med 1999;159:361-4.
10. Boutet K, Montani D, Jais X, Yaici A, Sitbon O, Simonneau G, et al. Therapeutic advances in pulmonary arterial hypertension. Ther Adv Respir Dis 2008;2:249-65.
11. Kouzu H, Nakatani S, Kyotani S, Kanzaki H, Nakanishi N, Kitakaze M. Noninvasive estimation of pulmonary vascular resistance by doppler echocardiography in patients with pulmonary arterial hypertension. Am J Cardiol 2009;103:872-6.
12. Chemla D, Castelain V, Herve P, Lecarpentier Y, Brimioulle S. Haemodynamic evaluation of pulmonary hypertension. Eur Respir J 2002;20:1314-31.
13. Segers P, Brimioulle S, Stergiopulos N, Westerhof N, Naeije R, Maggiorini M, et al. Pulmonary arterial compliance in dogs and pigs: The three-element windkessel model revisited. Am J Physiol 1999;277:H725-31.
14. Slife DM, Latham RD, Sipkema P, Westerhof N. Pulmonary arterial compliance at rest and exercise in normal humans. Am J Physiol 1990;258:H1823-8.
15. Rodes-Cabau J, Domingo E, Roman A, Majo J, Lara B, Padilla F, et al. Intravascular ultrasound of the elastic pulmonary arteries: A new approach for the evaluation of primary pulmonary hypertension. Heart 2003;89:311-5.
16. Berger RM, Cromme-Dijkhuis AH, Hop WC, Kruit MN, Hess J. Pulmonary arterial wall distensibility assessed by intravascular ultrasound in children with congenital heart disease: An indicator for pulmonary vascular disease? Chest 2002;122:549-57.
17. Fourie PR, Coetzee AR, Bolliger CT. Pulmonary artery compliance: Its role in right ventricular-arterial coupling. Cardiovasc Res 1992;26:839-44.
18. Piene H, Sund T. Does normal pulmonary impedance constitute the optimum load for the right ventricle? Am J Physiol 1982;242:H154-60.
19. Muthurangu V, Atkinson D, Sermesant M, Miquel ME, Hegde S, Johnson R, et al. Measurement of total pulmonary arterial compliance using invasive pressure monitoring and mr flow quantification during mr-guided cardiac catheterization. Am J Physiol Heart Circ Physiol 2005;289:H1301-6.
20. Hoskins PR, Hardman D. Three-dimensional imaging and computational modelling for estimation of wall stresses in arteries. Br J Radiol 2009;82:S3-17.
21. Tang BT, Fonte TA, Chan FP, Tsao PS, Feinstein JA, Taylor CA. Three-dimensional hemodynamics in the human pulmonary arteries under resting and exercise conditions. Ann Biomed Eng 2011;39:347-58.
22. Draney MT, Alley MA, Tang BT, Wilson NM, Herfkens RJ, Taylor CA. Importance of 3d nonlinear gradient corrections for quantitative analysis of 3d mr angiographic data Proceedings of the International Society for Magnetic Resonance in Medicine. Vol. 10. Tenth Scientific Meeting and Exposition; 2002.
23. Wilson NM, Wang K, Dutton RW, Taylor CA. A software framework for creating patient specific geometric models from medical imaging data for simulation based medical planning of vascular surgery. Lecture Notes in Computer Sci 2001;2208:449-56.
24. Wang KC, Dutton RW, Taylor CA. Level sets for vascular model construction in computational hemodynamics. IEEE EngMedBiol1999;18:33-9.
25. Taylor CA, Hughes TJ, Zarins CK. Finite element modeling of blood flow in arteries. Comput Methods Appl Mech Eng 1998;158:155-96.
26. Malek AM, Izumo S, Alper SL. Modulation by pathophysiological stimuli of the shear stress-induced up-regulation of endothelial nitric oxide synthase expression in endothelial cells. Neurosurgery 1999;45:334-44.
27. Noris M, Morigi M, Donadelli R, Aiello S, Foppolo M, Todeschini M, et al. Nitric oxide synthesis by cultured endothelial cells is modulated by flow conditions. Circ Res 1995;76:536-43.
28. Fisher AB, Al-Mehdi AB, Manevich Y. Shear stress and endothelial cell activation. Crit Care Med 2002;30:S192-7.
29. Galie N, Ghofrani HA, Torbicki A, Barst RJ, Rubin LJ, Badesch D, et al. Sildenafil citrate therapy for pulmonary arterial hypertension. N Engl J Med 2005;353:2148-57.
30. Furchgott RF, Zawadzki JV. The obligatory role of endothelial cells in the relaxation of arterial smooth muscle by acetylcholine. Nature 1980;288:373-6.
31. Ignarro LJ, Byrns RE, Buga GM, Wood KS. Endothelium-derived relaxing factor from pulmonary artery and vein possesses pharmacologic and chemical properties identical to those of nitric oxide radical. Circ Res 1987;61:866-79.
32. Murad F. The 1996 albert lasker medical research awards. Signal transduction using nitric oxide and cyclic guanosine monophosphate. JAMA 1996;276:1189-92.
33. Tzima E, Irani-Tehrani M, Kiosses WB, Dejana E, Schultz DA, Engelhardt B, et al. A mechanosensory complex that mediates the endothelial cell response to fluid shear stress. Nature 2005;437:426-31.
34. Chen BP, Li YS, Zhao Y, Chen KD, Li S, Lao J, et al. Dna microarray analysis of gene expression in endothelial cells in response to 24-h shear stress. Physiol Genomics 2001;7:55-63.
35. Garcia-Cardena G, Fan R, Shah V, Sorrentino R, Cirino G, Papapetropoulos A, et al. Dynamic activation of endothelial nitric oxide synthase by hsp90. Nature 1998;392:821-4.
36. Porreca E, Di Febbo C, Reale M, Castellani ML, Baccante G, Barbacane R, et al. Monocyte chemotactic protein 1 (mcp-1) is a mitogen for cultured rat vascular smooth muscle cells. J Vasc Res 1997;34:58-65.
37. Rieder MJ, Carmona R, Krieger JE, Pritchard KA Jr, Greene AS. Suppression of angiotensin-converting enzyme expression and activity by shear stress. Circ Res 1997;80:312-9.
38. McLaughlin VV, Genthner DE, Panella MM, Rich S. Reduction in pulmonary vascular resistance with long-term epoprostenol (prostacyclin) therapy in primary pulmonary hypertension. N Engl J Med 1998;338:273-7.

Source of Support: Dr. Tang was supported by the Benchmark Capital Fellowship in Congenital Cardiovascular Bioengineering. Drs. Feinstein and Tang were supported by the Vera Moulton Wall Center for Pulmonary Vascular Disease at Stanford, **Conflict of Interest:** None declared.